PHYSICAL REVIEW E **69**, 040801(R) (2004)

Stringlike structure formed in thin films of a lamella-forming diblock copolymer

Kenji Fukunaga*
UBE Industries, Ltd. 8-1 Goi-minamikaigan, Ichihara, Chiba 290-0045, Japan

Takeji Hashimoto†
Department of Polymer Chemistry, Graduate School of Engineering, Kyoto University, Kyoto 606-01, Japan
(Received 20 June 2003; published 14 April 2004)

Thin films of a lamella-forming polystyrene-*block*-poly(2-vinylpyridine) diblock copolymer, PS-P2VP, were annealed by a tetrahydrofuran (THF) vapor treatment. The thin films immediately developed a multilayered lamellar structure, similar to those known for conventional heat treatment. However, in the case of the vapor treatment, the steps moved over a significantly larger distance than the case of the heat treatment. This process strikingly developed stringlike objects (strings) that appeared near the steps. The strings were found to be cylindrical domains of poly(2-vinylpyridine) blocks (P2VP) partitioned from P2VP lamella during the step motion and sandwiched by the polystyrene phase that results in perforating the P2VP lamella. The string formation seemed to be associated with the motion of the step, which was considerably faster in the vapor treatment process than in the heat treatment process.

DOI: 10.1103/PhysRevE.69.040801 PACS number(s): 61.25.Hq, 61.41.+e, 68.55.Jk

Ordering process of the self-assembling materials, e.g., crystalline materials, generally traps nonequilibrium ''defects'' in the final structures. These defects closely relate to how the ordered structure has been formed. In this paper we will discuss our finding, the formation of an intriguing structure, a *stringlike structure*, in lamellar thin films of a symmetric diblock copolymer. As will be shown here, this string formation process is related to a moving of the steps formed on the free surface of the multilayered film, i.e., a change in the local thickness of the film involved by a dewetting process. The phenomena found in the block copolymer system may universally occur in the ordering of various smectic films comprised of liquid crystals, biomaterials, hydrogels, etc. [1].

The symmetric diblock copolymers comprised of two polymer chains covalently bonded at their chain ends are microphase-separated into lamellar morphologies in bulk [2]. In the case of the thin films, generally surfaces of the films selectively attract one of the block components and thereby induce alignment of the lamellar microdomains parallel to the surfaces (parallel lamellae) [3]. The block copolymer sample is frequently annealed above the highest glass transition temperature T_g of the constituents in order to establish an ordered equilibrium state from a distorted nonequilibrium structure (microphase-separated structures without long range order) formed in the preparation processes. On the other hand, treatment of the sample with vapor of a neutral solvent was explored recently [4,5]. In this treatment the swollen solvent decreases the T_g as well as the segregation power of the two components of the system. In thin films of a lamella-forming diblock copolymer, both the heat treatment and the solvent-vapor treatment cause thickness quantization with a stepped surface [see Figs. 1(a) and 1(b)]. However, in the case of the vapor treatment, the films significantly dewetted the substrate and thickened; the step move due to the film thickening was observed to occur over much larger distances than the heat treatment process. This may bring a new aspect to the self-assembly of the lamellar films that has not been encountered before in the heat treatment case.

Polystyrene-*block*-poly(2-vinylpyridine) diblock copolymer, PS-P2VP, used in this study has the number average molecular weight $M_n = 2.10 \times 10^5$ with a heterogeneity index of $M_w/M_n = 1.11$, where M_w is the weight-averaged molecular weight. The volume fraction of PS is 0.44. The bulk sample shows a lamellar structure with a spacing of 140 nm [6]. Thin films of the PS-P2VP were deposited onto a native oxide silicon (SiO_x) substrate from a 1 wt% solution of PS-P2VP in tetrahydrofuran (THF) by a dipping method. THF is a common solvent for polystyrene (PS) and poly(2-

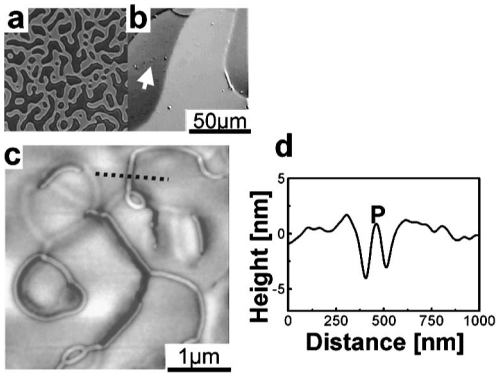

FIG. 1. Reflection optical micrograph of the PS-P2VP thin films on the SiO_x substrate developed by a heat treatment in vacuum at 210 °C for one week (a) and by the THF-vapor treatment for three days at room temperature (b). The 50 μm scale is common to both (a) and (b). (c) shows a SFM height image obtained at the position on the lower terrace as indicated by the arrow in (b). (d) represents the height profile along the dotted line in (c). Point P represents the center of the string.

*Email address: 28658u@ube-ind.co.jp
†Email address: hashimoto@alloy.polym.kyoto-u.ac.jp

vinylpyridine) (P2VP). The samples were exposed to saturated THF vapor in a closed chamber kept at room temperature. Ellipsometry determined a thickness and hence a degree of swelling in the films or the PS-P2VP concentration ϕ_P in the swollen films. The ϕ_P decreased to a steady value of about 40% after 10 min. At the end of the treatment, the samples were transferred to an atmosphere where the solvent was promptly evaporated.

The vitrified samples were observed by scanning force microscopy (SFM). TappingMode Nanoscope III (Digital Instruments, Santa Barbara, CA) was used for this purpose. The samples were investigated by transmission electron microscopy too with the electron beam parallel to the film plane (cross-sectional TEM). The PS-P2VP films were removed from the rigid SiO_x substrate [7] and put onto a polyimide substrate. After embedding in an UV-cured acrylic agent (Luxtrak, Toagosei Co., Tokyo, Japan), the samples were sliced, and stained by OsO_4 vapor. TEM images were taken on a JEM-200CX (JEOL, Japan) microscope operated at 100 kV.

The as-prepared PS-P2VP films had a uniform thickness of about 300 nm. Within the first 1 min of the vapor treatment, the thin films developed small areas (terraces) of well-defined interference color, though the image is not shown here. The color was stepwisely varied over the thin films, indicative of the thickness quantization which is well known for the system annealed by the heat treatment [3,8]. In contrast to the heat treatment, the boundaries of the terraces (steps) had been significantly moved during the vapor treatment. As a result of the step move, the terraces coarsened with time t during the treatment. The terrace coarsening seemed to be driven by a hydrodynamic flow within the lamellar film [9] rather than by a line tension [10]. The lateral dimension L of the terraces grows by roughly $L \sim Kt^{\alpha}$ and $\alpha = 0.55$ and $K = 0.4$ with L and t in units of micrometers and minutes, respectively. The prefactor K is several orders of magnitude larger than that found in the heat treatment [9]. At the same time, the film was dewetted from the substrate and thickened by forming higher terraces. The vapor treatment was stopped after three days. The solvent evaporation process did not change position of the steps significantly.

An optical microscopy image of the vapor-treated sample is shown in Fig. 1(b). Note that the vapor treatment developed much wider terraces than the heat treatment [see Fig. 1(a)]. A part of the lower terrace as indicated by the arrow in Fig. 1(b) is further inspected by SFM [Fig. 1(c)]. The height image shows that, surprisingly, the terrace is embedding stringlike objects (hereafter referred to as ''strings'') never observed in the case of the heat treatment. Each string is comprised of two parallel depressions with an interval of about 90 nm [see Fig. 1(d)]. A considerable number of the strings was observed on various areas of the sample. This finding is quite striking, since the terrace is expected to be composed of the parallel PS and P2VP lamellae which are laterally homogeneous.

Figure 2(a) shows a cross-sectional TEM micrograph of the sample. Here PS and P2VP domains are unstained and stained by OsO_4 and hence appear bright and dark, respectively. The sample is found to have parallel lamellar structure

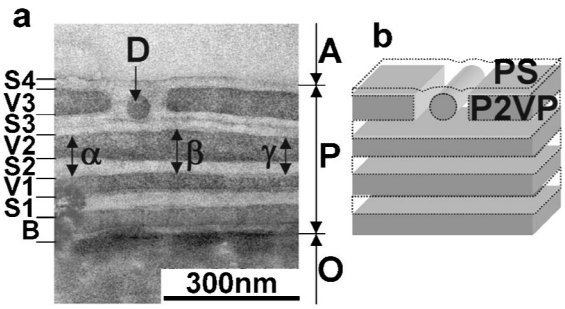

FIG. 2. Cross-sectional TEM image of the PS-P2VP thin film on the SiO_x substrate annealed by the THF vapor treatment for three days at room temperature (a). A, P, and O indicate embedding resin (hence corresponding to an air phase before the TEM preparation), the PS-P2VP film, and the substrate, respectively. An undulation of the lamella interfaces is highlighted by the difference between the spacing α to γ. (b) depicts schematically a model for the string indicated by D in (a). For the other markers, see text.

and to be composed of three P2VP full lamellae (V1–V3), three PS full lamellae (S1–S3), and two boundary layers (S4, B). The layer S4 on the free surface is composed of a half PS lamella. PS has a lower surface energy than P2VP, hence segregating to the free surface [11]. On the other hand, the boundary layer B on the substrate (O) is not simple, since the SiO_x surface strongly adsorbs P2VP chains and induced a special structure on the substrate surface, though we shall not elaborate on this further in this paper. The average lamella spacing is about 80 nm which is smaller than that observed in bulk (140 nm). It should be noted that the lamella interfaces are undulating as shown in the difference of the lamella spacing α, β, and γ in Fig. 2(a).

A remarkable finding is that, at the part indicated by D, the outmost PS domain (S4 and S3) perforates the P2VP lamella (V3) at two positions and, thereby, forms an isolated P2VP domain which appears as a round cross section. The perforations to P2VP lamella by the PS domain were observed at various positions of the sample. Interestingly, the PS domain perforates P2VP lamella always by the pair as observed in Fig. 2(a). The spacing between the pair PS perforations is about 90 nm, which is the same as the spacing between the two depressions in both sides of the string [Fig. 1(d)].

The depressions of ~ 5 nm in both sides of the strings as shown in Figs. 1(c) and 1(d) should be observed on the surface contour of the PS-P2VP film in Fig. 2(a). However, the depressions do not appear there, probably because they are so small in the scale of the figure. Nevertheless, we may possibly assume a model of the strings schematically shown in Fig. 2(b). In this model, the PS domain perforates P2VP lamella, leaving a P2VP cylinder in the PS matrix. Although THF is a common solvent of the system, it is slightly preferential to PS [12]. Therefore, during the THF-vapor treatment, the PS domain takes up more THF than the P2VP domain. After the solvent removal, the PS perforations are considered to shrink more than the area without the perforations, leaving the depressions of the free surface below which the PS perforations exist.

Now, a question is raised on how the P2VP string and the

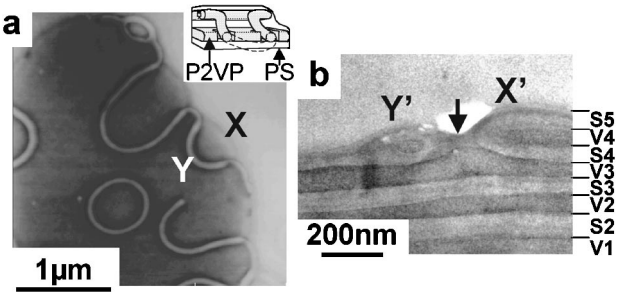

FIG. 3. (a) and (b) show a SFM height image taken near the step (X) and a cross-sectional TEM image of the corresponding portion (X′), respectively. The strings (e.g., Y) emanating from the step are observed in (a) and a correspondingly isolated micellar domain (Y′) appears in (b). A three-dimensional model of the string (Y or Y′) near the step is presented in the inset of (a).

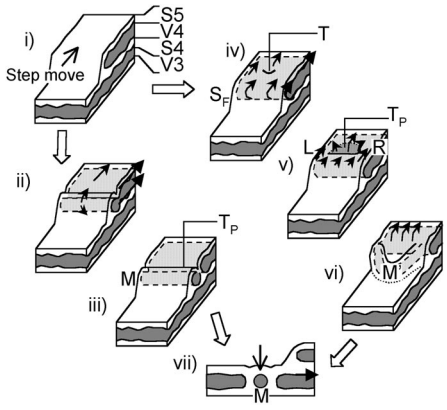

FIG. 4. Schematic diagram for the string formation process. See text for details.

pair PS perforations have developed. For lamella-forming dPS-P2VP, Liu *et al.* found cylinders created perpendicular to the steps in films less than 3/2 lamellar layers (see Fig. 4 in Ref. [13]). Our findings are different from theirs, since a significant number of the strings is generally observed even in thick films (more than three lamellar layers). However, the strings seemed not to be distributed randomly on the entire free surface. By inspecting in detail their locations, it turned out that the strings appear mostly near the steps. The probability density p of finding a part of the string from a curvilinear distance x from the step is roughly represented by $p = p_0 \exp(-x/l)$ and $l = 1.5$ μm (p_0 is a proportionality constant depending on the sampling area). The characteristic length l may be expressed by $v\tau$, where v is the velocity of the step and τ is the sustaining time of the string against the relaxation to the lamella.

An example is shown in Fig. 3(a). The height image shows a step between the lower (dark) and higher terraces (bright) with its height corresponding to the lamellar spacing as shown in Fig. 2(a). The strings are emanating from the higher step and exist on the lower terrace. Interestingly, they never exist on the higher terrace. PS-P2VP block copolymers that have different molecular weights also developed strings in thin films [6]. However, the lower (higher) M_n reduces (expands) the time scale τ_i of developing the strings. Furthermore, we found the τ_i increases with a decrease of the volume fraction of solvent brought by the reduction in the vapor pressure. It implies that the string formation may relate to the step move. Figure 3(b) shows a cross-sectional TEM image of the portion which corresponds to that shown in 3(a). X′ and Y′ seemingly correspond to X and Y in 3(a), respectively. The outmost P2VP lamella V4 is ended by an edge-dislocation type defect (X′) [3(b)]. In the left-hand part of X′, a P2VP cylindrical domain (Y′) is observed in the PS domain. Between X′ and Y′, the topmost PS layer (S5) merges to the subsequent PS layer (S4). The step accompanied by the dislocation (like X′) is moving during the vapor treatment due to the macroscopic dewetting and thickening of the thin film. Furthermore, in our system, the lamella interfaces are considerably undulating (e.g., see Fig. 2). The string formation may be attributed to this undulated interface and the step move. We assume the following scenario for the string formation: the moving step (containing the defect like X′) develops the micelle (like Y′), and the micelle is transformed to the string.

The schematic diagram of Fig. 4(i) shows a step moving toward the backside of the space (the direction indicated by the arrow) accompanied by the dewetting and thickening of the thin film. The lamellae with undulating interfaces are thinner in some parts, and thicker in some parts, than the mean spacing. In order for the step to move junction points of block copolymers may diffuse and flow due to either of the following two cases. In the first case [part (ii)], the junction points on both the interface between V4 and S5 and that between V4 and S4 diffuse and flow along the direction of the step move (as indicated by the two arrows). This case will decrease the junction-point density around the tip of V4 because the driving force for the junction points to diffuse and flow on the two interfaces described above is balanced at the tip. This causes the necking of V4 near the tip and separates a P2VP micelle [M in part (iii)] from the P2VP lamella V4 [see the process shown from parts (i) to (iii)]. On the other hand, in the second case [part (iv)], the junction points diffuse and flow in such a way that the diffusion rolls up the interface around the V4 tip. When the step approaches the thinner area (indicated by T) of V4, the flow of junction points is slowed down in front of T and this part of the P2VP domain may be compressed. On the other hand, in the backside of T, this compression is relaxed, the flow tends to be accelerated, and this part tends to be pulled up. This flow tends to make T thinner and eventually part of T will be perforated [see the region T_P in part (v)]; the T region may be elongated parallel to the step front [S_F defined in part (iv)]. In part (v) the perforation should inhibit the flow of the junction points across T_P, though the flow still occurs on both sides of the T_P region (L and R) where the V4 domain is not yet perforated. When the step front comes close to T_P, the flow should deform the step front S_F of the V4 domain and the perforated T_P region, developing a core-shell micelle M [in part (vi)] with a P2VP core and a PS shell. As the step moves further, this micelle is left on the lower terrace (vii). In both cases of parts (iii) and (vi), the protruded micelle M has an excess surface area and costs a free energy penalty. In order to minimize the surface free energy, M will be embed-

ded in the lamella as shown in the process of parts (iii) or (vi) and (vii). The diffusion of the junction points in the layer V3 is associated with this process. The micelle embedded in the lamella will be observed as the string. This string M is interconnected to the V4 lamella as schematically illustrated in the three-dimensional model shown in the inset of Fig. 3(a).

In Fig. 3(a) the strings touch the step tangentially and extend down toward the lower terrace, implying that the strings have been formed in the step and they have been left by the step move described above. By inspecting the trajectory of the protruded part P of the string [defined in the height profile across the string shown in Fig. 1(d)] along its longitudinal direction for many strings, it was revealed that the height of P relative to the lower terrace surface h is a monotonically decreasing function of a curvilinear distance x from the steps, confirming the model suggested in the inset to Fig. 3(a). The function is roughly approximated by $h=h_0-\alpha x$ in the range $200\ \mathrm{nm}<x<1000\ \mathrm{nm}$ with $\alpha=7\times 10^{-3}$ and $h_0=8$ nm. Both short strings and long strings are embedded in the lower terrace [see Figs. 3(a) and 1(c)], indicating that both of the cases of Figs. 4(ii) and 4(iv) may account the string formation. These pieces of experimental evidence seem to support the aforementioned scenario of the string formation. When the solvent is slowly removed so that the steps move during the drying process, the solvent removal may influence the string formation.

Since the lamella-forming block copolymers are in the same universality class with the smectic liquid crystals, the strings may form in the case of the smectic liquid crystal films too. In the liquid crystal films, the steps are believed to move significantly fast. This meets the condition presented in the string formation scenario. However, relaxation of the strings is also fast which may make observation of the strings difficult. In spite of it, some particular textures observed in the free-standing thin films of the smectic liquid crystals [14] may relate to the defect formation similar to that discussed here. On the other hand, the strings may form in lamella-forming more complicated block copolymer systems as well, like the one studied in Ref. [5]. In this case, the chain connectivity and cooperative diffusion and flow of the many types of junctions appear to prolong the time scale of developing the strings, which makes the observation of the strings much easier than the smectic liquid crystals of small molecules.

In conclusion, we found stringlike objects (strings) in thin films of a lamella-forming diblock copolymer when the films were annealed by the solvent-vapor treatment. The films formed a parallel lamellar structure, which was similar to the case of the heat treatment. However, in the case of the vapor treatment, the surface steps moved over much larger distances than those developed in the case of the heat treatment. The large step move and the undulation of the lamella interfaces near the step seem to be primarily responsible for the formation of the strings.

[1] Y. Bouligand, *Handbook of Liquid Crystals* (Wiley-VCH Verlag, Weinheim, 1998), Vol. 1.
[2] I. Hamley, *Physics of Block Copolymers* (Oxford University Press, Oxford, 1998), Vol. 94.
[3] G. Coulon, V.R. Deline, P.F. Green, and T.P. Russell, Macromolecules **22**, 2581 (1989).
[4] R.J. Albalak, M.S. Capel, and E.L. Thomas, Polymer **39**, 1647 (1998).
[5] K. Fukunaga, T. Hashimoto, H. Elbs, and G. Krausch, Macromolecules **35**, 4406 (2002).
[6] K. Fukunaga and T. Hashimoto (unpublished).
[7] P. Mansky, Y. Liu, E. Huang, T.P. Russell, and C.J. Hawker, Science **275**, 1458 (1997).
[8] T.P. Russell, G. Coulon, V.R. Deline, and D.C. Miller, Macromolecules **22**, 4600 (1989).
[9] J. Heier, E. Sivaniah, and E.J. Kramer, Macromolecules **32**, 9007 (1999).
[10] P. Bassereau, D. Brodbreck, T.P. Russell, H.R. Brown, and K.R. Shull, Phys. Rev. Lett. **71**, 1716 (1993).
[11] H. Hasegawa and T. Hashimoto, Macromolecules **18**, 589 (1985).
[12] H. Elbs, K. Fukunaga, R. Stadler, G. Sauer, R. Magerle, and G. Krausch, Macromolecules **32**, 1204 (1999).
[13] Y. Liu, M.H. Rafailovich, J. Sokolov, S.A. Schwarz, and S. Bahal, Macromolecules **29**, 899 (1996).
[14] P. Cluzeau, G. Joly, H.T. Nguyen, C. Gors, and V.K. Dolganov, Phys. Rev. E **62**, R5899 (2000).